The FASEB Journal • Research Communication

Activation of EPAC1/2 is essential for osteoclast formation by modulating NFκB nuclear translocation and actin cytoskeleton rearrangements

Aránzazu Mediero, Miguel Perez-Aso, and Bruce N. Cronstein[1]

Department of Medicine, Division of Translational Medicine, New York University School of Medicine, New York, New York, USA

ABSTRACT **Bisphosphonates inhibit osteoclast differentiation/function *via* inhibition of Rap1A isoprenylation. As Rap1 is the effector of exchange protein directly activated by cAMP (EPAC) proteins, we determined the role of EPAC in osteoclast differentiation. We examined osteoclast differentiation as the number of primary murine/human bone-marrow precursors that differentiated into multinucleated TRAP-positive cells in the presence of EPAC-selective stimulus (8-pCTP-2′-O-Me-cAMP, 100 μM; 8-pCTP-2′-O-Me-cAMP-AM, 1 μM) or inhibitor brefeldin A (BFA), ESI-05, and ESI-09 (10 μM each). Rap1 activity was assessed, and signaling events, as well as differentiation in EPAC1/2-knockdown RAW264.7 cells, were studied. Direct EPAC1/2 stimulation significantly increased osteoclast differentiation, whereas EPAC1/2 inhibition diminished differentiation (113±6%, $P<0.05$, and 42±10%, $P<0.001$, of basal, respectively). Rap1 activation was maximal 15 min after RANKL stimulation (147±9% of basal, $P<0.001$), whereas silencing of EPAC1/2 diminished activated Rap1 (43±13 and 20±15% of control, $P<0.001$) and NFkB nuclear translocation. TRAP-staining revealed no osteoclast differentiation in EPAC1/2-KO cells. Cathepsin K, NFATc1, and osteopontin mRNA expression decreased in EPAC1/2-KO cells when compared to control. RhoA, cdc42, Rac1, and FAK were activated in an EPAC1/2-dependent manner, and there was diminished cytoskeletal assembly in EPAC1/2-KO cells. In summary, EPAC1 and EPAC2 are critical signaling intermediates in osteoclast differentiation that permit RANKL-stimulated NFkB nuclear translocation and actin rearrangements. Targeting this signaling intermediate may diminish bone destruction in inflammatory arthritis.—Mediero, A., Perez-Aso, M., Cronstein, B. N. Activation of EPAC1/2 is essential for osteoclast formation by modulating NFκB nuclear translocation and actin cytoskeleton rearrangements. *FASEB J.* 28, 4901–4913 (2014). www.fasebj.org**

Key Words: RhoA · cdc42 · Rac1 · FAK

Osteoclasts, multinucleated giant cells derived from myeloid precursors belonging to the monocyte/macrophage family (1, 2), resorb bone during normal bone remodeling and, by increasing in number and resorptive capacity, mediate pathological bone loss, as well. Osteoclasts adhere to bone and form a sealing zone into which they secrete HCl and proteases, such as collagenases, cathepsin K, and tartrate-resistant acid phosphatase (TRAP), which dissolve the mineral and matrix components of bone (3). Myeloid precursors differentiate into osteoclasts after stimulation by macrophage colony-stimulating factor 1 (M-CSF), which acts *via* its receptor CSF-1R. After interaction with M-CSF, differentiation and activation of osteoclasts is mediated by a complex network of regulatory factors (systemic hormones and locally produced cytokines) and cell–cell and cell–matrix interactions that are required for transition of the osteoclast precursor into a multinucleated and fully activated osteoclast (4, 5). Among these factors, receptor activator of nuclear factor κ-B ligand (RANKL) is a critical extracellular regulator of osteoclast differentiation and activation (6–10). RANKL binds to its receptor, RANK, on the surface of osteoclast precursors (OCPs), resulting in the recruitment of TNF receptor associated factors (TRAFs), which activate nuclear factor κB (NFκB), c-Fos, phospholipase Cγ (PLCγ), and nuclear factor of

Abbreviations: 8-pCTP-2′-O-Me-cAMP, 8-(4-chlorophenylthio)-2′-*O*-methyladenosine-3′,5′-cyclic monophosphate; 8-pCTP-2′-O-Me-cAMP-AM, 8-(4-chlorophenylthio)-2′-*O*-methyladenosine-3′,5′-cyclic monophosphate acetoxymethyl ester; BMC, bone marrow cell; BFA, brefeldin A; EPAC, exchange protein directly activated by cAMP; ESI-05, 4-methylphenyl-2,4,6-trimethylphenylsulfone; ESI-09, 3-[5-(*tert*-butyl)isoxazol-3-yl]-2-[2-(3-chlorophenyl)hydrazono]-3-oxopropanenitrile; FAK, focal adhesion kinase; KO, knockout; M-CSF, macrophage colony-stimulating factor 1; NFATc1, nuclear factor of activated T cells c1; NFκB, nuclear factor κB; PKA, protein kinase A; qRT-PCR, quantitative reverse transcriptase-polymerase chain reaction; RANKL, receptor activator of nuclear factor κ-B ligand; TRAP, tartrate-resistant acid phosphatase

[1] Correspondence: Division of Translational Medicine, Department of Medicine, New York University School of Medicine, 550 First Ave., MSB251, New York, NY 10016, USA. E-mail: bruce.cronstein@nyumc.org

doi: 10.1096/fj.14-255703

This article includes supplemental data. Please visit *http://www.fasebj.org* to obtain this information.

activated T cells c1 (NFATc1) to induce differentiation of OCPs into osteoclasts (5).

One of the major messenger pathways involved in regulating osteoclast formation is adenylate cyclase/cAMP. cAMP signals by activating protein kinase A (PKA) and exchange proteins activated by cAMP (EPAC), a family of proteins that comprises EPAC1 and EPAC2 (11). The role of PKA in osteoclast differentiation has been extensively studied, but the precise role of PKA activation in osteoclast differentiation remains uncertain. Recent data suggest that PKA and increased cAMP activate (12) osteoclastogenesis. cAMP analogs mimicked the effect of PGE2 (13), where osteoclast differentiation occurs in combination with 1,25-(OH)1D3, and is induced *via* cAMP-dependent PKA (14). Moreover, it has been reported that RANKL-induced degradation of IκBα and phosphorylation of p38 MAPK and c-Jun N-terminal kinase in RAW264.7 cells are up-regulated by PGE_2 in a cAMP/PKA-dependent fashion (15). In addition, estrogens suppress PTH-stimulated osteoclast-like cell formation by blocking both the cAMP-dependent PKA pathway and the PLC-coupled calcium/PKC pathway (16). In contrast, several reports described the inhibitory effect of PKA activation on osteoclastogenesis and root resorption by odontoclasts (17, 18). Pretreatment with adenosine 3′,5′-cyclic monophosphothioate Rp diastereomer (Rp-cAMPS), a PKA inhibitor, suppressed the calcitonin-induced inhibition of actin-ring formation. Moreover, calcitonin, through cAMP/PKA/EPAC cascades, inhibits osteoclast formation, an effect that is not associated with decreased transcription of genes known to be important for osteoclast progenitor cell differentiation, fusion or function (19). Inhibition of PKA exerts its antiresorptive effects on osteoclasts, in part by reducing lysosomal pools of catalytically active cathepsin K (20) and therefore reducing processing and maturation in osteoclasts. Finally, we have recently reported that adenosine A_{2A} receptors signal for inhibition of NFκB translocation to the nucleus and inhibit osteoclast differentiation by a mechanism that involves cAMP-PKA-ERK1/2 signaling (21).

Although EPAC signaling is also downstream of adenylate cyclase/cAMP generation, little has been reported on the role of EPAC in osteoclast differentiation. Zou *et al.* (22) have shown that Rap1 is critical for resorptive function, and its selective inhibition in mature osteoclasts retards pathological bone loss (22). Previous work has demonstrated that one mechanism by which bisphosphonates inhibit osteoclast differentiation and function is *via* inhibition of Rap1A (an effector of the cAMP-binding EPAC protein) isoprenylation and function (23–25). Inhibition of osteoclast differentiation by calcitonin was mimicked not only by compounds activating cAMP and PKA but also by a cAMP analog activating the EPAC pathway (19).

To better understand the role of EPAC1/2 in suppression or stimulation of osteoclast differentiation, we examined the effect of RANKL-induced osteoclast differentiation on EPAC1/2 activation and the downstream effects of this stimulation on critical signaling steps in osteoclast differentiation.

MATERIALS AND METHODS

Reagents

RAW264.7 cells were from American Type Culture Collection (ATCC; Manassas, VA, USA). Recombinant mouse M-CSF and recombinant mouse RANKL were from R&D Systems (Minneapolis, MN, USA). α-MEM, FBS, penicillin/streptomycin and Alexa Fluor 555 phalloidin were from Invitrogen (Life Technologies, NY, USA). Sodium acetate, glacial acetic acid, naphthol AS MX phosphate disodium salt, fast red violet LB, RIPA buffer, protease inhibitor cocktail, phosphatase inhibitor cocktail, hexadimethrine bromide, brefeldin A (BFA), lentivirus packing particles (scrambled, EPAC1 and EPAC2), puromycin selection marker, and Fluoroshield with DAPI mounting medium were from Sigma-Aldrich (St. Louis, MO, USA). Sodium tartrate was from Fisher Scientific (Pittsburgh, PA, USA). 8-(4-chlorophenylthio)-2′-*O*-methyladenosine-3′,5′-cyclic monophosphate (8-pCTP-2′-O-Me-cAMP), 8-(4-chlorophenylthio)-2′-*O*-methyladenosine-3′,5′-cyclic monophosphate acetoxymethyl ester (8-pCTP-2′-O-Me-cAMP-AM), 4-methylphenyl-2,4,6-trimethylphenylsulfone (ESI-05), and 3-[5-(*tert*-butyl)isoxazol-3-yl]-2-[2-(3-chlorophenyl)hydrazono]-3-oxopropanenitrile (ESI-09) were from Biolog Life Science Institute (San Diego CA, USA). Rabbit polyclonal anti-actin (sc-130656), rabbit polyclonal anti-p-RhoA (sc-32954), mouse monoclonal anti-RhoA (sc-418), rabbit polyclonal anti-Rac1 (sc-217), and rabbit polyclonal anti-cdc42 (sc-87) were from Santa Cruz Biotechnology (Santa Cruz, CA, USA). Rabbit polyclonal anti-NFκB p50/p105 (ab32360), rabbit polyclonal anti-IκBα (ab32518), rabbit polyclonal anti-p-IκBα (ab93141), rabbit polyclonal anti-focal adhesion kinase (FAK; ab4803), and mouse monoclonal anti-nuclear matrix protein p84 (ab487) were from Abcam (Cambridge, MA, USA). NE-PER nuclear and cytoplasmic extraction reagents kit and BCA Protein Assay Reagent were from Thermo Scientific (Pierce Protein Research Products, Rockford, IL, USA). Rap1 activation assay kit was from Millipore (EMD Millipore Chemicals, Philadelphia, PA, USA). CellTiter96 aqueous nonradioactive cell proliferation assay and CytoTox96 nonradioactive cytotoxicity assay were from Promega (Madison, WI, USA).

Transfection protocol

EPAC1 and EPAC2 shRNA transfection was performed as described previously (21). Briefly, 15,000 RAW264.7 cells were plated, and 24 h later, cells were incubated in the presence of hexadimethrine bromide (4 μg/ml) and 10^8 lentiviral transduction particles corresponding to mouse EPAC1 (RAPGEF3, SHCLNV-NM_144850, 5′-CCGGAGGTGTTGGTGAAGGTCAATTCTCGAGAATTGACCTTCACCAACACCTTTTTTG-3′) and EPAC2 (RAPGEF4, SHCLNV-NM_019688, 5′-CCGGGAGTTATGTACGGCAATTAAACTCGAGTTTAATTGCCGTACATAACTCTTTTTTG-3′), with puromycin selection marker, for another 24 h to allow transfection. Medium was then replaced with αMEM containing puromycin (1 μg/ml), changing the medium every 3 d until selected clones formed. These clones were isolated and expanded until confluent. Scrambled shRNA (SHC002V) was used as a control. Permanently silenced clones are kept in culture under puromycin selection.

Osteoclast differentiation

The New York University School of Medicine Institutional Animal Care and Use Committee (IACUC) approved all protocols related to animals. Bone marrow cells (BMCs) were isolated from 6–8 wk old female C57BL/6 mice as described previously (26). Briefly, the marrow cavity was flushed out with α-MEM from femora and tibiae that was aseptically removed, and bone marrow was incubated overnight in α-MEM containing 10% FBS and 1% penicillin/streptomycin (α-MEM) to obtain a single-cell suspension. Next, 200,000 nonadherent cells were collected and seeded in a 48-well plate in α-MEM with 30 ng/ml M-CSF for 2 d. At d 3 (d 0 of differentiation), 30 ng/ml RANKL was added to the culture in the presence of EPAC activators 8-pCTP-2′-O-Me-cAMP (100 μM) and 8-pCTP-2′-O-Me-cAMP-AM (1 μM), and the inhibitors BFA (10 μM), ESI-05 (10 μM), and ESI-09 (10 μM) (n=6/assay). Cultures were fed every third day by replacing the culture medium with fresh medium and reagents. Next, 5000 EPAC1- and EPAC2-transfected RAW264.7 cells (shRNA EPAC1, shRNA EPAC2; or scrambled shRNA as control) were differentiated in a 48-well plate in with 50 ng/ml RANKL (n=5/assay). Human bone marrow myeloid precursors were separated by Ficoll density gradient using Histopaque-1077 according to the manufacturer's instructions, and 200,000 cells were seeded in in a 48-well plate in α-MEM with 30 ng/ml M-CSF for 2 d. At d 3 (d 0 of differentiation), 30 ng/ml RANKL was added to the culture in the presence of 8-pCTP-2′-O-Me-cAMP (100 μM) or BFA (10 μM) (n=4 each assay). RAW264.7 cells were used before the sixth passage.

After incubation of mouse and human BMCs for 7 or 3 d (RAW264.7 cells), cells were prepared for TRAP staining for osteoclast quantification (21, 26). The number of TRAP-positive MNCs containing ≥3 nuclei/cell was scored (27). All cell counts were carried out by individuals who were blinded to the sample identity. In all experiments, DMSO is added to the control at the same concentration, as it is present in conditions containing various agonists and antagonists.

To assay resorption activity, 5000 shRNA EPAC1 and shRNA EPAC2 RAW264.7 cells (or scrambled shRNA as control) were seeded on dentine slides (Immunodiagnostic Systems, Scottsdale, AZ, USA) in α-MEM with 50 ng/ml RANKL (n=4/assay). After 3 d of differentiation, resorption was assayed by staining the dentine slides with 1% toluidine blue in 0.5% sodium tetraborate solution, following the manufacturer's recommendations. The pits developed blue to purple color. Numbers of pits are expressed as means ± SD.

Osteoclast proliferation assay

CellTiter96 aqueous nonradioactive cell proliferation assay kit was used to study cell proliferation in primary cultures in the presence of 8-pCTP-2′-O-Me-cAMP (100 μM) or BFA inhibitor, and in shRNA EPAC1 and EPAC2 cells (n=6 each). A 96-well plate was seeded with 5000 cells, and the cells were treated with 30 ng/ml RANKL (or 50 ng/ml for the shRNA cells) for 48 h alone or in the presence of 8-pCTP-2′-O-Me-cAMP (100 μM) or BFA (10 μM). Proliferation was analyzed following the manufacturer's protocol.

Osteoclast cytotoxicity assay

CytoTox96 nonradioactive cytotoxicity assay kit was used to study 8-pCTP-2′-O-Me-cAMP and BFA cytotoxicity. For this, 5000 primary cells and shRNA EPAC1 and EPAC2 cells were seeded in a 96-well plate and treated with 30 ng/ml RANKL (or 50 ng/ml for the shRNA cells) for 48 h alone or in the presence of 8-pCTP-2′-O-Me-cAMP (100 μM) or BFA (10 μM) (n=6 each). Cytotoxicity was analyzed following the manufacturer's protocol.

Morphological characterization of cultured osteoclasts

Osteoclasts were generated from shRNA EPAC1 and shRNA EPAC2 RAW264.7 cells (or scrambled shRNA as control). To differentiate osteoclasts, transfected RAW264.7 cells were plated at 7500 cells/ml on fibronectin-coated glass coverslips (Lab-Tek II chamber slide, 8-well; Nalge Nunc International, Penfield, NY, USA) in α-MEM containing 50 ng/ml RANKL (n=4/assay). After 3 d in culture, cells were fixed with 4% paraformaldehyde in PBS, blocked with PBS 1% BSA 0.1% Triton X-100 for 30 min, stained fluorescently with Alexa Fluor 555 Phalloidin for 30 min and counterstained with DAPI as described previously (28). To evaluate osteoclast morphology, averages of 400 osteoclasts were examined in each sample using confocal microscopy (Leica SP5 confocal system; Leica Microsystems, Wetzlar, Germany).

cAMP measurements

Intracellular cAMP was measured with the Amersham cAMP Biotrak enzyme immunoassay system (Amersham, Arlington Heights, IL, USA) using the nonacetylation EIA procedure, following the protocol. Briefly, 100,000 RAW264.7 cells were plated in a 96-well plate and incubated with 50 ng/ml RANKL for different time points (n=6 each) and the recommended protocol was followed. Optical density was read at 450 nm, and results were calculated as described by the manufacturer.

Rap1 activation assay

Ninety percent confluent shRNA EPAC1 and shRNA EPAC2 RAW264.7 cells (or scrambled shRNA as control) in 100 mm culture wells were stimulated for 15 min with 50 ng/ml RANKL. Rap1 activation assays using a GST-tagged fusion protein corresponding to aa 788–884 of the human Ral-GDS-Rap binding domain bound to glutathione agarose (Ral GDS-RBD agarose) were performed using a Rap1 activation assay kit (Millipore) according to the manufacturer's directions (n=4). After lysing cells in Rap1 activation lysis buffer, one sample (scrambled cells) was incubated with GTPγS as a positive control, and the other sample (scrambled cells also) was incubated with GDP as a negative control. Rap1 was pulled down in all samples using Ral GDS-RBD slurry, and Rap1 was detected by SDS-PAGE and Western blot analysis. Total Rap1 was used as a control.

Western blot analysis

For Western blot analysis of NFκB nuclear translocation and actin cytoskeleton, EPAC1 and EPAC2 shRNA-transfected RAW264.7 cells (shRNA EPAC1 and shRNA EPAC2; or scrambled shRNA as control) were activated with 50 ng/ml of RANKL (n=4 each), collected at different time points, and lysed with RIPA buffer containing protease/phosphatase inhibitors to extract total cell protein content. Cytoplasmic and nuclear fraction protein extraction was performed using NE-PER nuclear and cytoplasmic extraction reagent kits (Thermo Scientific). Protein concentration was determined by BCA. Next, 4 μg of protein was subjected to 7.5 or 10% SDS-PAGE and transferred to a nitrocellulose membrane. To block nonspecific binding, membranes were treated in TBS/0.05% Tween-20 with 5%

skim milk for 1 h at room temperature, and were incubated overnight at 4°C with primary antibodies against p50/p105 NFκB (1:5000), IκBα (1:500), and p-IκBα (1:500), pRhoA (1:1000), FAK (1:1000), cdc42 (1:1000), and Rac1 (1:1000). After washing with TBS/0.05%Tween-20, membranes were incubated with goat anti-rabbit IRDye 800CW (1:10000) and goat anti-mouse IRDye 680 RD (1:10,000) (Li-Cor Biosciences, Lincoln, NE, USA) for 1 h at room temperature in the dark. Proteins were visualized by Li-Cor Odyssey equipment where near-infrared fluorescent signals were detected, as each secondary antibody emits a signal in a different spectrum. The blots were then reprobed with actin or RhoA (to check that all lanes were loaded with the same amount of protein) at the same time as the primary antibody incubation. Specific nuclear signal was detected using mouse monoclonal antinuclear matrix protein p84 (diluted 1:1000). Intensities of the respective band were quantitated by densitometric analysis using the Image Studio 2.0.38 software (Li-Cor Biosciences).

To quantify the Western blots, digital densitometric band analysis was performed, and band intensities were expressed relative to actin, RhoA, or p84, as appropriate. Variations in intensity were expressed as percentage of control and are reported as means ± SD. All results were calculated as a percentage of nonstimulated controls to minimize the intrinsic variation among different experiments. Statistical analysis was performed by 1-way ANOVA and Bonferroni posttest. Levels of significance are indicated in the figure legends.

Real-time quantitative reverse transcriptase-polymerase chain reaction (qRT-PCR)

To confirm the function of EPAC1 and EPAC2 in osteoclast differentiation modulation, we measured the activation of the two osteoclast differentiation markers, cathepsin K and NFATc1, and osteopontin, an extracellular structural protein that initiates the development of osteoclast ruffled borders, in EPAC1 and EPAC2 shRNA-transfected RAW264.7 cells (and scrambled shRNA for control) activated with 50 ng/ml of RANKL (n=4/assay) by qRT-PCR as described previously (26). Briefly, cells were collected during the 3 d of differentiation and total RNA was extracted using RNeasy Mini Kit (Qiagen, Invitrogen) including sample homogenization with QIAshredder columns. On-column DNA digestion was performed to avoid genomic DNA contamination. Total RNA (0.5 μg) was retrotranscribed using the MuLV RT-PCR kit (Applied Biosystems, Foster City, CA, USA) at 2.5 U/μl, including in the same reaction Rnase inhibitor (1 U/μl), random hexamers (2.5 U/μlm), $MgCl_2$ (5 mM), PCR buffer II 1×, and dNTPs (1 mM). Real-time PCR was used for relative quantification of gene expression using a Stratagene Mx3005P (Agilent Technologies, La Jolla, CA, USA) with Brilliant Fast SYBR Green Kit qPCR Master Mix (Stratagene). The following primers were used: cathepsin K, forward 5′-GCTGAACTCAGGACCTCTGG-3′, reverse 5′-GAAAAGGGAGGCATGAATGA-3′; *NFATc1*, forward 5′-TCATCCTGTCCAACACCAAA-3′, reverse 5′-TCACCCTGGTGTTCTTCCTC-3′; osteopontin, forward 5′-tctgatgagaccgtcactgc-3′, reverse 5′-tctcctggctctctttggaa-3′; and GAPDH, forward 5′-CTACACTGAGGACCAGGTTGTCT-3′, reverse 5′-GGTCTGGGATGGAAATTGTG-3′. The Pfaffl method (29) was used for relative quantification of cathepsin K, NFATc1, and osteopontin.

Statistical analysis

Statistical significance for differences between groups was determined by use of 1-way ANOVA and the Bonferroni posttest. All statistics were calculated using GraphPad software (GraphPad, San Diego, CA, USA).

RESULTS

RANKL stimulates EPAC activation

As previously reported (12, 13, 21), when osteoclast precursor cells are stimulated with 50 ng/ml RANKL, there is a time-dependent increase in intracellular cAMP levels, reaching a maximum 5–10 min after RANKL stimulation (**Fig. 1*A***). Previously, we have demonstrated that both PKA-selective cAMP analogues 8-Cl-cAMP and 6-Bnz-cAMP (100 nM) inhibited osteoclast differentiation, whereas the selective PKA inhibitor (PKI) increased osteoclast differentiation (21). Because cAMP signals *via* activation of both PKA and EPAC, we sought to determine the role of direct EPAC activation in osteoclast differentiation.

The EPAC-selective cAMP analog, 8-pCTP-2′-O-Me-cAMP (100 μM), enhanced osteoclast differentiation induced by RANKL alone in primary murine BMCs cells (113±6% of basal, P<0.05, n=6), whereas the EPAC inhibitor BFA diminished osteoclast differentiation (42±10% of basal, P<0.001, n=6) (Fig. 1*A*). We studied the effects of the same agents on primary human BMCs and found substantially identical results (Fig. 1*B*); 8-pCTP-2′-O-Me-cAMP increased the number of TRAP positive cells when compared to RANKL alone (117±8% of basal, P<0.05, n=6), whereas BFA inhibited osteoclast differentiation (35±11% of basal, P<0.001, n=6). Moreover, we observed the same results in osteoclast differentiation in RAW264.7 cells for 8-pCTP-2′-O-Me-cAMP and BFA (Supplemental Fig. S1*A*). Because the effects of these signaling pathway agents were identical in both the murine cell line and primary cells, we carried out the remainder of these studies with the RAW264.7 cell line.

Due to the possibility that 8-pCTP-2′-O-Me-cAMP may not penetrate cells fully, and to further confirm the role of EPAC in osteoclast differentiation, we studied osteoclast differentiation in the presence of the AM-ester form of 8-pCTP-2′-O-Me-cAMP, and the newly reported inhibitors of EPAC activation (ESI-05 and ESI-09). As shown in Supplemental Fig. S1*B*, the AM-ester increased osteoclast differentiation by 20% (P<0.05, n=6). Both ESI-05 and ESI-09 completely blocked RANKL-induced osteoclast differentiation (Supplemental Fig. S1*B*). Moreover, a partial rescue in osteoclast differentiation was observed when stably transduced cells lacking (10% of control) EPAC1 and EPAC2 expression were challenged with 8-pCTP-2′-O-Me-cAMP-AM (Supplemental Fig. S1*B*).

To confirm the pharmacologic evidence for involvement of EPAC in osteoclast differentiation, we knocked down both members of the EPAC family, EPAC1 and EPAC2, by infecting RAW264.7 cells with lentiviral particles containing shRNA for EPAC1 or EPAC2, and selected the relevant infected cells with puromycin. As

a control, we infected cells with vector containing scrambled shRNA. Both EPAC1 and EPAC2 protein and mRNA expression were knocked down by 80 to 90% (Supplemental Fig. S2). As observed in Fig. 1*D*, silencing of either EPAC1 or EPAC2 prevents RANKL-induced osteoclast differentiation (5±3 and 3±5% of control osteoclast formation, respectively; $P<0.001$, $n=4$). 8-pCTP-2′-O-Me-cAMP-AM (1 μM) partially rescued osteoclast differentiation in the EPAC1- and EPAC2-knockdown cells (Supplemental Fig. S1*B*).

We further investigated the involvement of EPAC1/2 in bone resorption *in vitro*. Morphometric measurement of toluidine blue-stained dentine slides clearly demonstrated a marked reduction in number of pits formed by RANKL when EPAC1 or EPAC2 was knocked down (11±5 for shRNA EPAC1, 12±6 for shRNA EPAC2, compared to 148±15 for scrambled shRNA; $P<0.001$, $n=4$; Fig. 1*E*).

To confirm that neither 8-CPT-cAMP, BFA, EPAC1 silencing, nor EPAC2 silencing had any effect on cell proliferation or were cytotoxic, both proliferation (Fig. 1*F*) and cytotoxicity (Fig. 1*G*) were analyzed. As we can observe, 48 h after primary cells were challenged with RANKL in the presence of 8-CPT-cAMP or BFA, no changes in proliferation were observed when compared to RANKL alone or nonactivated cells (Fig. 1*F*). Neither silence of EPAC1 or EPAC2 affected cell proliferation when compared to scrambled shRNA-infected RAW 264.7 cell proliferation (Fig. 1*F*). Neither 8-CPT-cAMP, BFA, EPAC1 silencing, nor EPAC2 silencing were cytotoxic when compared to untreated cells (Fig. 1*G*).

To confirm that EPAC1 and EPAC2 knockdown inhibits osteoclast differentiation, we determined the expression of mRNA for markers of osteoclast differentiation in these cells. As shown in Fig. 1*H*, treatment of RAW264.7 cells infected with scrambled shRNA with 50 ng/ml RANKL increased the expression of mRNA for cathepsin K (by up to 4.6±2-fold change on d 3; $P<0.001$, $n=4$), an effect that was abrogated in EPAC1 and EPAC2 shRNA-expressing cells (Fig. 1*H*). The same behavior was found for NFATc1 mRNA expression: RANKL increased NFATc1 mRNA expression to up 3 ± 1.2-fold on d 3 of differentiation ($P<0.01$; $n=4$; Fig. 1*D*), and this up-regulation was lost when either EPAC1 or EPAC2 were knocked down. Finally, mRNA expression for osteopontin was also increased in the RANKL-stimulated RAW264.7 cells (scrambled cells) by up to 3 ± 0.7-fold change on d 3 ($P<0.001$, $n=4$), and knockdown of both EPAC1 and EPAC2 prevented the RANKL-mediated increase in mRNA levels (Fig. 1*H*).

RANKL mediated EPAC activation mediates the activation of the Ras-like small GTPase Rap1

To determine whether the osteoclast activation of EPAC1/2 by RANKL proceeded *via* activation of the Ras-like small GTPase Rap1, we directly studied Rap1 activation in both shRNA EPAC1 and EPAC2 RAW264.7 cells (and scrambled shRNA cells as control). As shown in **Fig. 2**, RANKL treatment increased Rap1 activation, with maximal change observed 15 min after stimulation (147±9% of basal; $P<0.001$, $n=4$). The increase in Rap1 activation is diminished in cells in which either EPAC1 or EPAC 2 was knocked down (43±13 and 20±15% of control, respectively; $P<0.001$, $n=4$; Fig. 2).

EPAC activation mediates osteoclast differentiation by NFκB nuclear translocation

Activation and translocation of NFκB to the nucleus are required steps in osteoclast differentiation (21, 30) so we therefore determined whether EPAC signaling is required for p105/p50 NFκB nuclear translocation. As shown in **Fig. 3**, and as described previously, RANKL stimulates a rapid (15 min) and significant increase in p50/p105 NFκB nuclear translocation (135±9% of control; $P<0.001$, $n=4$), concomitant with a decrease in cytoplasmic p50/p105 NFκB (31±8% decreased; $P<0.001$, $n=4$) in scrambled RAW264.7 cells. We also found a decrease in cellular IκBα (63±9% decrease; $P<0.001$, $n=4$) with an increase in phosphorylated IκBα (177±12% of control; $P<0.01$, $n=4$) 5 min after stimulation. Silencing of both EPAC1 and EPAC2 blocked NFκB translocation, with an increase in cytoplasmic p50/p105 NFκB (120±9 and 150±115% of control, respectively; $P<0.001$, $n=4$), a decrease in nuclear p50/p105 NFκB (53±7 and 35±9% of control, respectively; $P<0.001$, $n=4$) (**Fig. 4**), concomitant with an increase in cellular IκBα (115±8 and 155±11% of control, respectively; $P<0.05$ and $P<0.001$, respectively, $n=4$) and a decrease in p-IκBα (83±4 and 95±4% of control, respectively; $P<0.05$ and not significant, respectively, $n=4$) (Fig. 3).

EPAC activation mediates osteoclast differentiation by modulation of actin cytoskeleton rearrangements

During osteoclast maturation, there is rearrangement of the actin cytoskeleton that is required for osteoclast differentiation and function (26, 28). As previously shown, osteoclasts cultured on glass show 3 distinct morphologies (Fig. 4*A* and ref. 26): an early stage of least mature osteoclasts (small with centrally located nuclei surrounded by a ring of F-actin and absent of podosomes; Fig. 4*A*, (arrow A); an intermediate stage of maturing osteoclasts (variable in size, dendritic shaped, and contain >5 nuclei with podosomes in patches and connected with other maturing cells through cytoplasmic bridges; Fig. 4*A*, arrow B); and the late stage of mature osteoclasts (large multinucleated with a peripheral podosome belt; Fig. 4*A*, arrow C). In culture, RANKL stimulates a marked increase in the number of mature osteoclasts when compared to maturing and least mature osteoclasts in scrambled shRNA RAW264.7 cells (74±9, 12±3, and 17±4% of total osteoclasts at each stage, respectively; $P<0.001$, $n=4$; Fig. 4*B*, *C*). When EPAC1 was knocked down, the differentiation of mature osteoclasts was almost completely blocked (69±9% least mature, 35±4% maturing, and 2±1% mature of total osteoclasts, respectively; $P<0.001$, $n=4$),

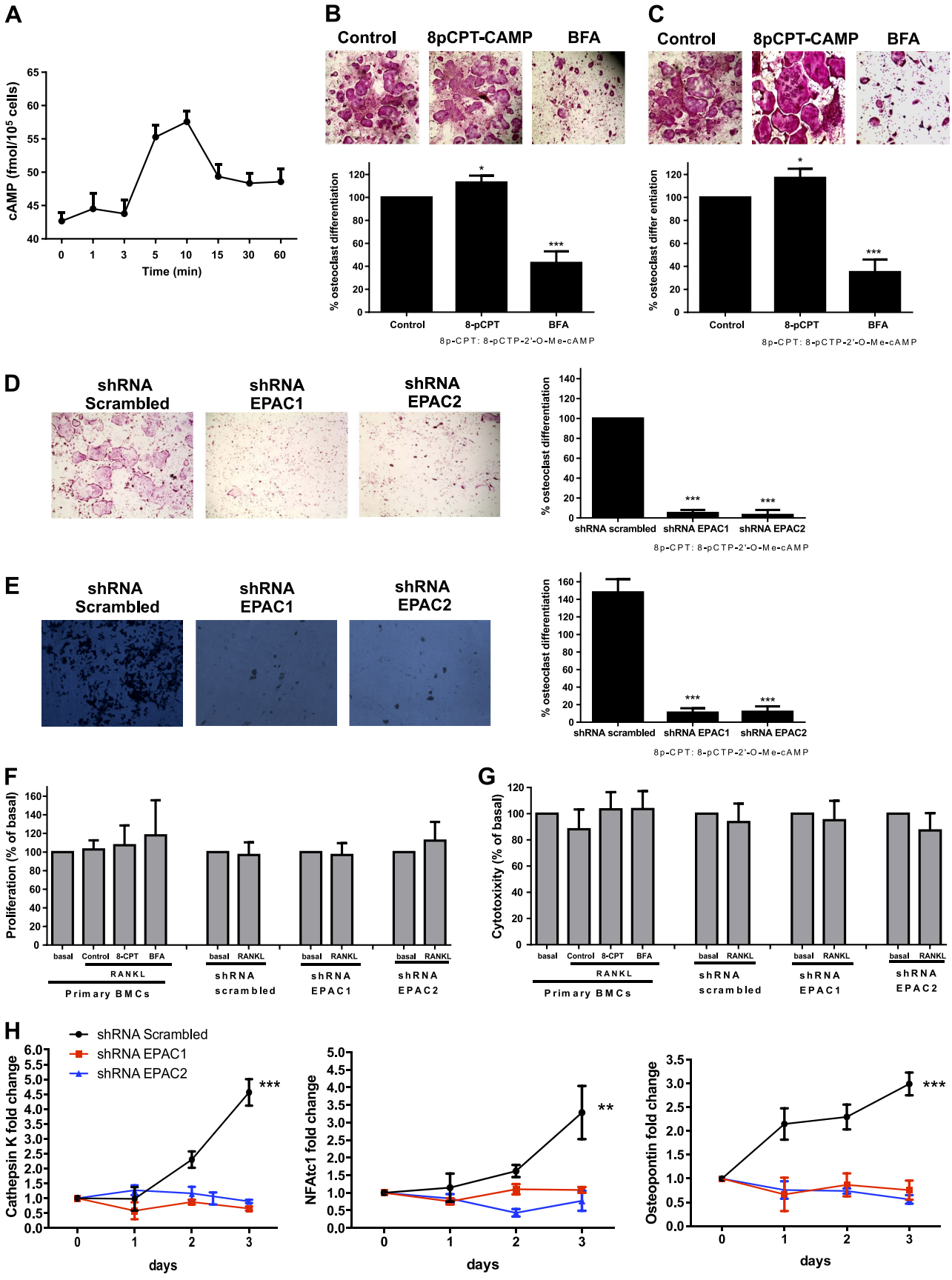

Figure 1. EPAC1 and EPAC2 are essential for osteoclast differentiation. *A*) Cellular cAMP levels over time following stimulation with 50 ng/ml RANKL. cAMP values are expressed as means ± SD (n=6). *B*) Mouse BMCs treated with 30 ng/ml RANKL together with 8-pCTP-2′-O-Me-cAMP or BFA were fixed and stained for TRAP. TRAP+ cells containing ≥3 nuclei were counted

(*continued on next page*)

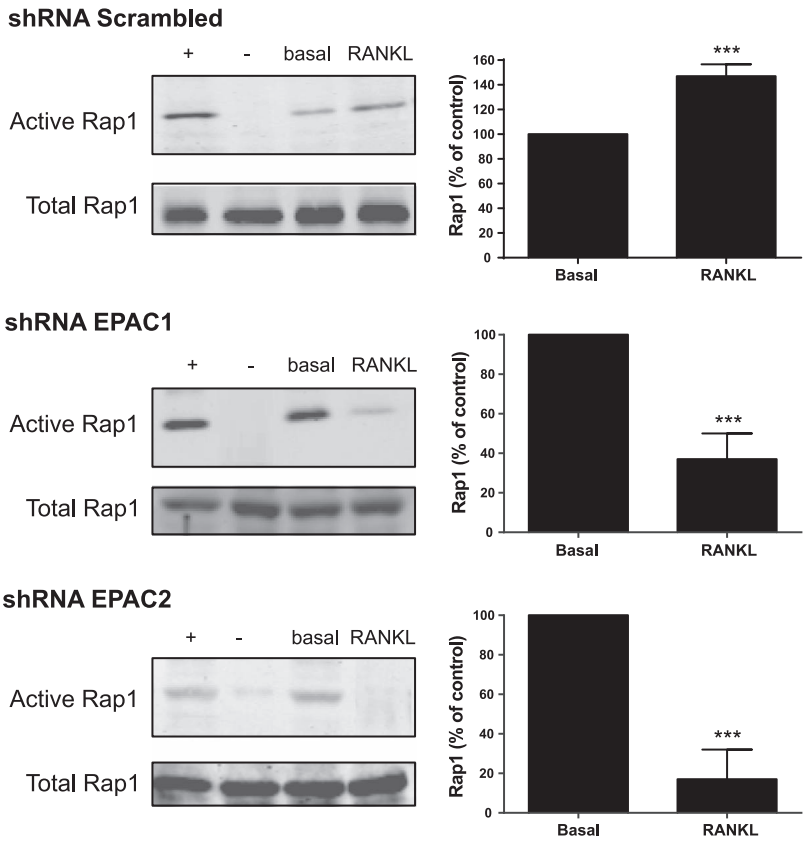

Figure 2. RANKL-mediated EPAC activation mediates the expression of the Ras-like small GTPase Rap1. RAW264.7 cells were stably transduced with scrambled or EPAC1 and EPAC2 shRNA and treated with 50 ng/ml RANKL. At 15 min after stimulation, Rap1 pulldown assay was performed, as described in Materials and Methods. Representative Western blots of activated and corresponding total Rap1 protein are shown. Summary data are expressed as mean ± SD percentage of activated Rap1 (percentage of nonstimulated cells; $n=4$). + indicates positive control; − indicates negative control. $^{**}P < 0.01$, $^{***}P < 0.001$ *vs.* nonstimulated control.

and similar results were observed when EPAC2 was knocked down (76±6% least mature, 28±3% maturing, and 1±1% mature of total osteoclasts, respectively; $P<0.001$, $n=4$) (Fig. 4*B*, *C*).

Because EPAC proteins and their downstream mediator, Rap1, are involved in cytoskeleton assembly, we examined the role of EPAC proteins in actin cytoskeleton changes. We studied changes in phosphorylation of RhoA (regulates the actin cytoskeleton in the formation of stress fibers) along with activation of cdc42 (regulates actin polymerization to induce the assembly of filopodia), Rac1 (drives actin polymerization and formation of lamellipodia and promotes cell-cell adhesion) and FAK (involved in cellular adhesion), as these proteins play important roles in osteoclast morphology and function by regulating the cytoskeleton (31). As shown in **Fig. 5*A***, and as described previously, RhoA phosphorylation is increased by RANKL in scrambled shRNA control cells (160±10% of basal; $P<0.001$, $n=4$), an effect completely abrogated when both EPAC1 and EPAC2 were knocked down (90±13 and 100±8% of basal, respectively; not significant, $n=4$). Similar results were found for cdc42; RANKL stimulated an increase in cdc42 expression (120±9% of basal; $P<0.05$, $n=4$) in control cells but not in cells in which EPAC2 was knocked down (102±6% of basal; not significant, $n=4$) (Fig. 5*B*). cdc42 expression was diminished when EPAC1 was knocked down (65±10% of basal; $P<0.01$, $n=4$; Fig. 5*B*). RANKL increased Rac1 expression (120±7% of basal; $P<0.01$, $n=4$) and this increase was inhibited when both EPAC1 and EPAC2 were knocked down (75±11 and 70±8% of basal, respectively; $P<0.05$, $n=4$) (Fig. 5*C*). Finally, FAK activation was increased in control cells after stimulation

as osteoclasts. *C*) Primary human BMC-derived osteoclasts were fixed and stained for TRAP following the same conditions as primary cells. *D*) RAW264.7 cells were stably transduced with scrambled or EPAC1 and EPAC2 shRNA, and the number of RANKL-induced osteoclasts was studied by TRAP staining. *E*) RAW264.7 cells were stably transduced with scrambled or EPAC1 and EPAC2 shRNA and treated with 50 ng/ml RANKL. Toluidine blue staining was performed to assay osteoclast activity. Results are expressed as mean ± SD number of pits formed. *F*) Primary cells were challenged with 30 ng/ml RANKL in the presence of 8-pCTP-2′-O-Me-cAMP or BFA, and proliferation was analyzed 48 h later. EPAC1- and EPAC2-knockdown cells were challenged for 48 h with 50 ng/ml RANKL, and proliferation was analyzed. Results are expressed as percentage of basal levels. *G*) Primary cells were challenged with 30 ng/ml RANKL in the presence of 8-pCTP-2′-O-Me-cAMP or BFA, and cytotoxicity was analyzed 48 h later. EPAC1- and EPAC2- knockdown cells were challenged for 48 h with 50 ng/ml RANKL, and cytotoxicity was analyzed. Results are expressed as percentage of basal levels. *H*) RAW264.7 cells were stably transduced with scrambled or EPAC1 and EPAC2 shRNA and treated with 50 ng/ml RANKL. Changes in cathepsin K, NFATc1, and osteopontin mRNA during the 3 d osteoclast differentiation process in EPAC1 and EPAC2 shRNA RAW264.7 cells were compared to scrambled shRNA-infected cells. All results are expressed as means ± SD ($n=6$). $^{*}P < 0.05$, $^{**}P < 0.01$, $^{***}P < 0.001$ *vs.* nonstimulated control.

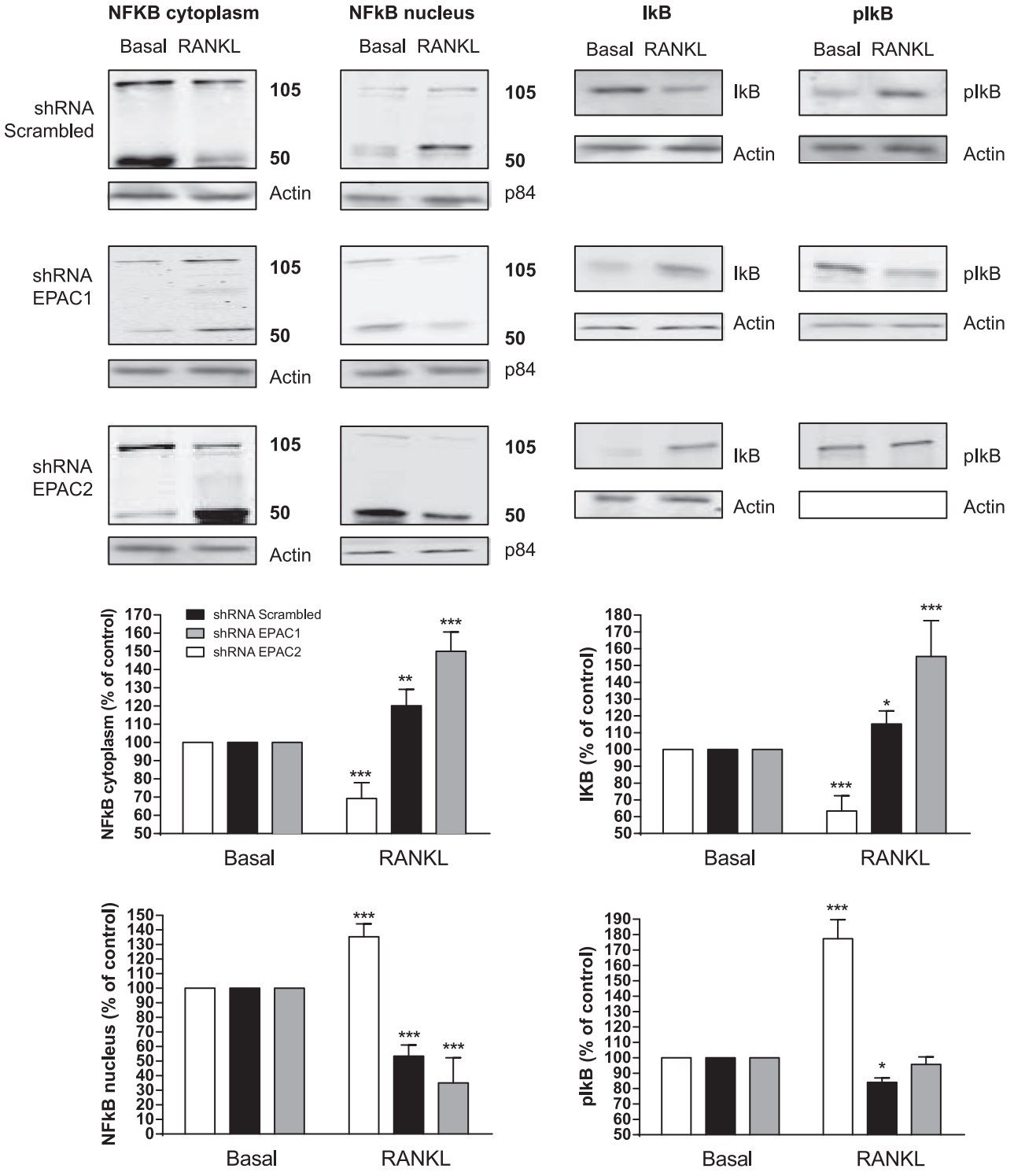

Figure 3. EPAC activation promotes NFκB p50/p105 nuclear translocation. EPAC1, EPAC2, and scrambled silenced RAW264.7 cells were treated with 50 ng/ml of RANKL and p50/p105 NFκB in the cytoplasmic and nuclear cell fractions, IκBα and p-IκBα were studied by Western blot. Results are expressed as means ± SD of 4 independent experiments. To normalize for protein loading, the membranes were reprobed for actin or p84, respectively, and results normalized appropriately. *Y* axis has been expanded to show the differences more clearly. $^*P < 0.05$, $^{***}P < 0.001$ *vs.* nonstimulated control.

with RANKL (149±13% of basal; $P<0.001$, $n=4$) but not in EPAC1-knockdown cells (101±5% of basal; not significant, $n=4$) (**Fig. 6*B***). FAK activation was inhibited when EPAC2 was knocked down (76±9% of basal; $P<0.05$, $n=4$; Fig. 5*D*).

As a result, we can conclude that direct activation of EPAC1/2 is required for RhoA phosphorylation and is essential for cdc42 activation. Also, direct activation of Rac1 and FAK is necessary for actin cytoskeleton rearrangements during osteoclast differentiation (Fig. 6).

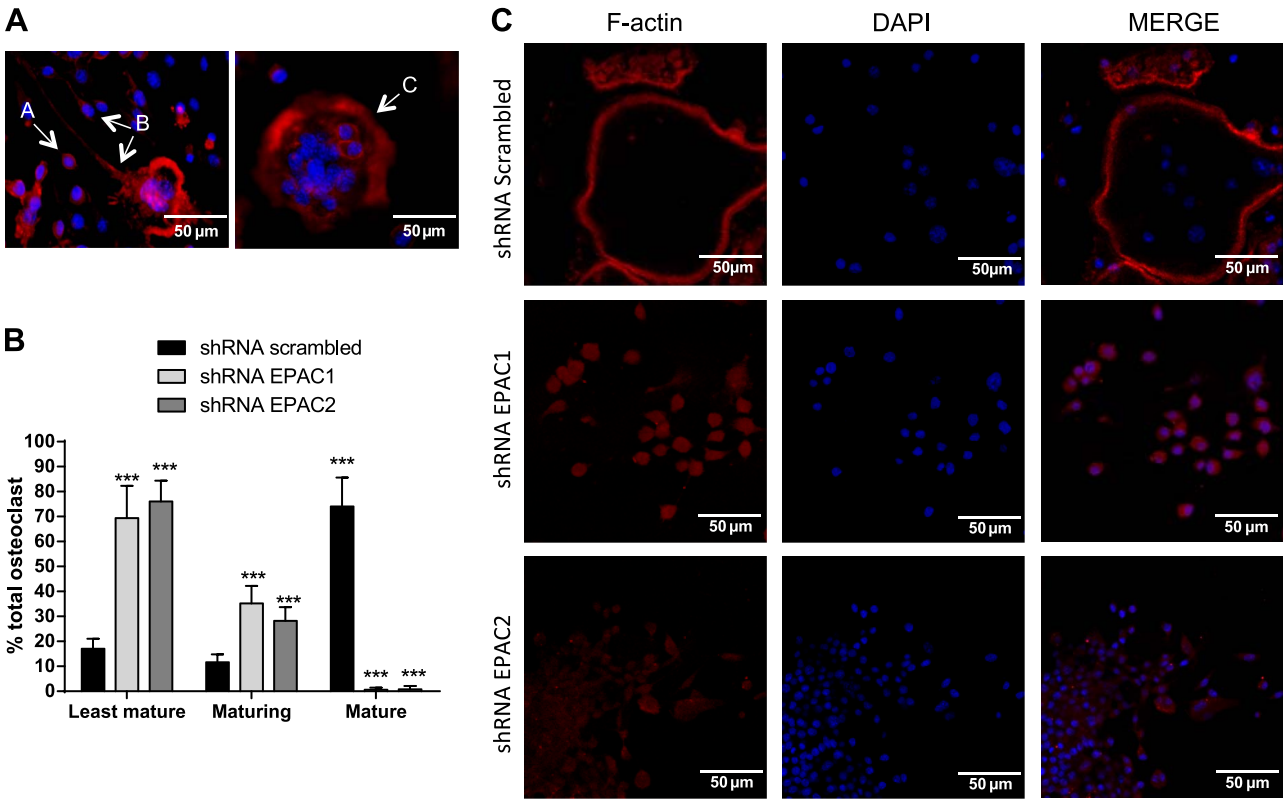

Figure 4. Morphological characterization of osteoclast cultures. *A*) F-actin was detected by Alexa 555-Phalloidin staining. Osteoclasts cultured on glass show 3 distinct morphologies: early stage of least mature osteoclasts (arrow A); an intermediate stage of maturing osteoclasts (arrow B), and the late stage of mature osteoclasts (arrow C). *B*) RAW264.7 cells stably transduced with EPAC1, EPAC2, or scrambled shRNA were treated with 50 ng/ml of RANKL for 3 d. Cells were plated in fibronectin-coated glass coverslips, and quantitative evaluation of number of least mature, maturing, and mature osteoclasts in osteoclast cultures in EPAC1, EPAC2, and scrambled silenced RAW264.7 cells was performed. Results are expressed as means ± SD of 4 independent experiments. *C*) F-actin was detected by Alexa 555-phalloidin staining. Images were taken at an original view of ×63. $*P < 0.05$, $**P < 0.01$, $***P < 0.001$ *vs.* scrambled cells.

DISCUSSION

The involvement of cAMP and PKA in osteoclast differentiation has been extensively studied, although the roles of these signaling intermediates in osteoclast differentiation remain controversial. Some studies suggest that cAMP formation and PKA activation by PTH activate osteoclastogenesis (12), and that cAMP analogs mimicked the effect of PGE2 in osteoclast differentiation (13–16). In contrast, others report that PKA activation exerts an inhibitory effect on osteoclastogenesis and root resorption by odontoclasts (17–21, 32). Our results suggest that these divergent results may result from activation of EPAC1 and EPAC2 as well as PKA by cAMP. EPAC1 and EPAC2 are expressed in many tissues, such as the brain, blood vessels, kidney, adrenal gland, and pancreas (14) where they play a role in signaling for a variety of cellular functions and processes, such as neuronal signaling or vascular permeability, cell proliferation, and insulin secretion (33). Because investigation into the roles of EPAC1/2 began much more recently, it is likely that many discrepant results in the field of cAMP signaling can now be explained by unexpected effects of EPAC1/2.

Previous work has demonstrated that bisphosphonates inhibit osteoclast differentiation and function by inhibition of Rap1A (effector of the cAMP-binding EPAC protein) isoprenylation and function (34). In the prior literature, there was no direct demonstration that EPAC1/2 played a role in osteoclast differentiation; however, Granholm (19) reported that an EPAC-selective cAMP analog mimics the inhibitory effects of calcitonin and other compounds that activate cAMP in osteoclast differentiation. Interestingly, these compounds did not affect transcription of genes known to be important for osteoclast differentiation. One possible explanation for the discrepancy between these previously published results and those reported here is that the EPAC-selective analogues are not completely selective for EPAC, and because high concentrations of these compounds are required to achieve a pharmacologic effect, there may be other off-target effects, as well. In our studies, we demonstrated a direct effect of EPAC1/2 stimulation by 2 different cAMP analogues, inhibition of EPAC1/2 by 3 different EPAC1/2 inhibitors, and lentiviral shRNA-mediated knockdown on osteoclast differentiation associated with activation of genes known to be important for osteoclast differenti-

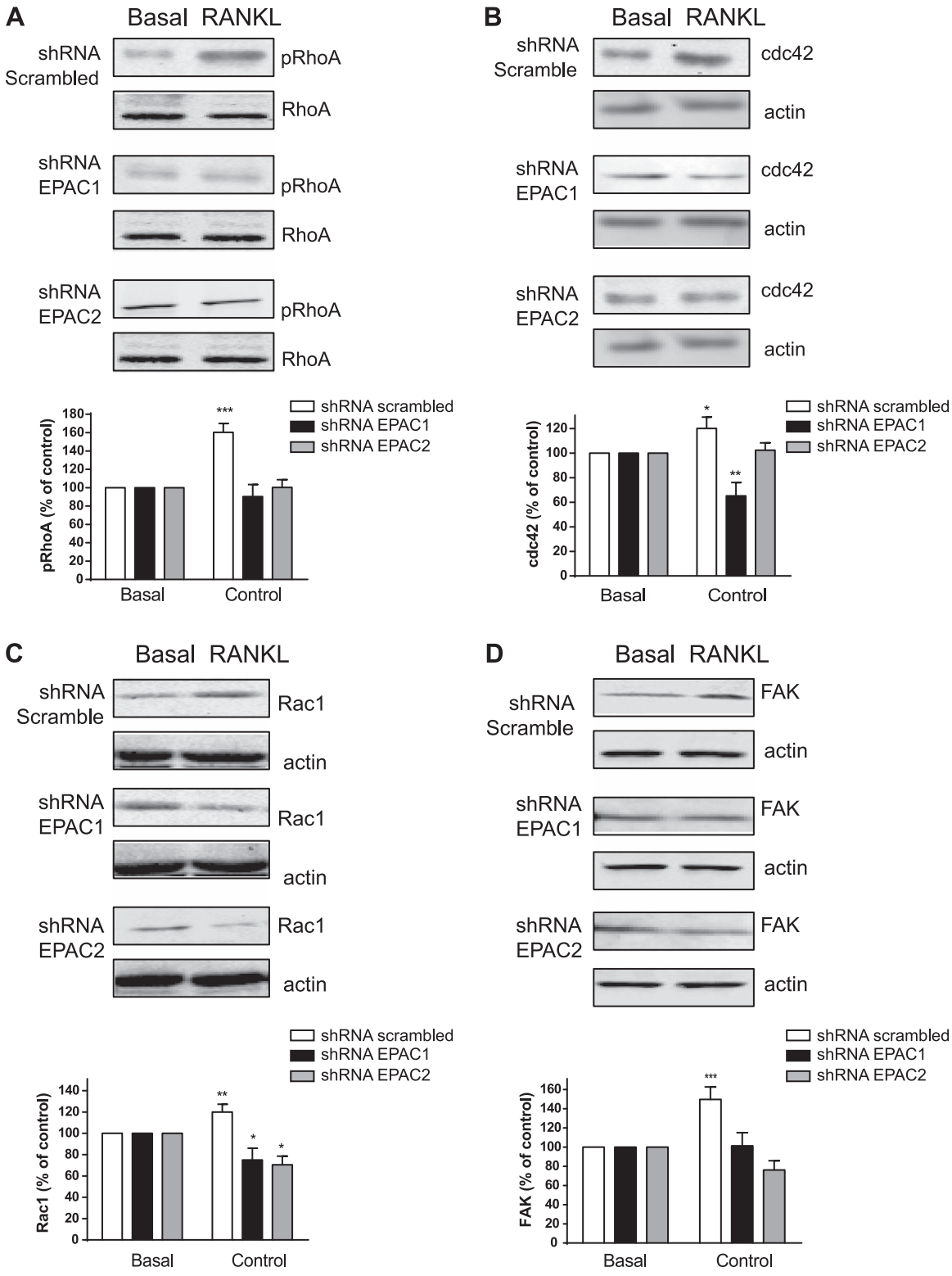

Figure 5. EPAC activation promotes RhoA phosphorylation and cdc42 activation. RAW264.7 cells stably transduced with shRNA for EPAC1, EPAC2, or scrambled were treated with 50 ng/ml of RANKL for 15 min. Western blots are representative. *A*) RhoA phosphorylation was analyzed by Western blot. *B*) cdc42 activation was studied by Western blot. *C*) Rac1 activation was analyzed by Western blot. *D*) FAK activation was studied by Western blot. Results are expressed as mean ± SD of 4 independent experiments. To normalize for protein loading, the membranes were reprobed with actin and results normalized appropriately. $*P < 0.05$, $***P < 0.001$ *vs.* nonstimulated control.

ation, and we found an important role for EPAC1/2 in osteoclast differentiation and activation of important pathways for osteoclast differentiation and function.

We were surprised to find that RANKL stimulation leads to an increase in cAMP generation that is sufficient to activate EPAC1/2. This finding suggests the

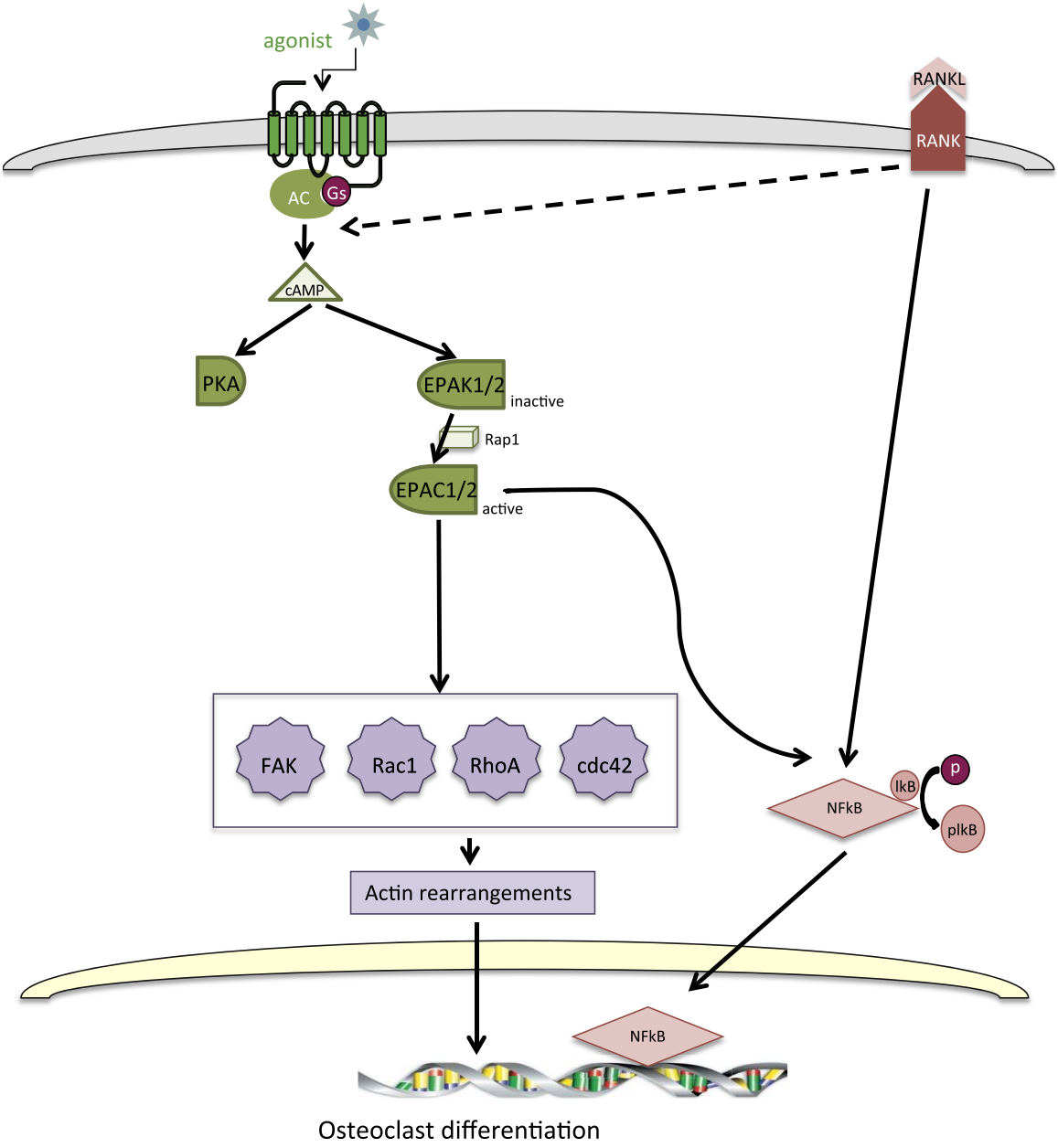

Figure 6. cAMP activation of EPAC promotes osteoclast differentiation by p50/p105 NFκB nuclear translocation and actin rearrangements. Activation of EPAC by the G_s-coupled receptor mediated by RANKL/RANK activation results in activation of p50/p105 NFκB nuclear translocation and the actin cytoskeleton. These events result in promotion of osteoclast differentiation.

following signaling pathway for promotion of osteoclast differentiation by RANKL: cAMP stimulates EPAC1 and EPAC2, which activate a guanine nucleotide exchange factor (GEF) for the Ras-like small GTPase Rap1 (13), which, in turn, activates MAPKinases and NFκB nuclear translocation and induces assembly of the actin cytoskeleton, leading to osteoclast differentiation (Fig. 6).

As described previously, the classical NFκB pathway is critical for osteoclast differentiation and function (16, 32, 35, 36). Thus, mice lacking the p50 subunit of NFκB do not generate osteoclasts, and p50 and p52 double-knockout (KO) mice have shortened long bones, and there are no TRAP-positive osteoclasts in bone (30). Moreover, the NBD peptide (inhibitor of the classical NFκB pathway) blocks the bone-resorbing activity of osteoclasts by reducing area, volume, and depths of pits, reducing TRAP activity, disrupting actin rings, and preventing osteoclast migration (36). In this work, we have demonstrated that direct activation of EPAC1/2 promotes p50 NFκB nuclear translocation, an effect that is abrogated when either of the EPAC proteins is knocked down. This may indicate that both EPAC proteins may be activated in order to promote p50 NFκB nuclear translocation.

Osteoclasts exhibit two different actin cytoskeleton organizations according to their substratum. On non-mineralized substrates, they form podosomes, and on mineralized extracellular matrices, they form a sealing

zone. Dynamic actin remodeling is a critical step during osteoclast differentiation (26, 28, 31, 37), and we have found that knockdown of both EPAC1 and EPAC2 prevents direct activation of RhoA, cdc42, Rac1, and FAK proteins by EPAC1/2, as well as actin remodeling. This observation may indicate that RhoA, cdc42, Rac1, and FAK are necessary for actin cytoskeleton rearrangements during osteoclast differentiation activation by EPAC1/2 (Fig. 6). Our results correlate with previous results in which cdc42 mediates bone resorption principally by stimulating osteoclastogenesis, although in that report Rac meaningfully affects the differentiation of osteoclasts, as Rac1 and Rac2 are mutually compensatory (38). Others have observed that inhibition or activation of Rho and Rac activities leads to complete disorganization of fibrillar actin structures, including podosomes, as these are extremely unstable structures, and any changes of Rho or Rac activity result in their dissociation (39). Moreover, loss of FAK results in reduced bone resorption by osteoclasts *in vitro*, coincident with impaired signaling through the CSF-1R (40). Our results also correlate with previous results that indicate a direct effect in actin rearrangements and cAMP activation. It has been reported that the calcitonin-induced inhibition of osteoclast function is due to disruption of cytoskeletal organization and disappearance of the cellular polarity of osteoclasts in a cAMP-PKA- and Ca^{2+}-PKC-dependent mechanism (41). A relation between cAMP/PKA/EPAC and actin cytoskeleton has also been found in other systems, for example, activation with 8-Br-cAMP stimulates [^{14}C]-α-methyl-D-glucopyranoside uptake *via* EPAC and PKA-dependent sodium-glucose cotransporter expression and trafficking through caveolin-1 and F-actin in renal proximal tubule cells (42). Activation of EPAC by G_s-coupled receptors alters actin dynamics and the microtubule network in lung cells, thereby modulating diverse processes, including cell migration, cell division, cell adhesion, and cell proliferation (43).

In summary, EPAC1/2 is a critical intermediate in osteoclast differentiation that permits NFkB nuclear translocation and actin rearrangements. Targeting this signaling intermediate may diminish bone destruction in inflammatory arthritis. FJ

This work was supported by grants from the U.S. National Institutes of Health (AR56672, AR56672S1, AR54897, AR046121), the New York University–Health and Hospitals Corp. Clinical and Translational Science Institute (UL1TR000038), a New York University Caregiver Intervention Center Support grant (9NIH/NCI 5 P30CA16087-310), and grants from OSI (Melville, NY, USA), Takeda (Deerfield, IL, USA), and Gilead Pharmaceuticals (Foster City, CA, USA). A.M. and B.N.C. have filed a patent on use of adenosine A_{2A}R agonists to prevent prosthesis loosening (U.S. patent 8,183,225), and have filed a patent on use of antinetrin-1 antibodies for the treatment of bone disease (pending). M.P-A. declares no conflicts of interest. B.N.C. holds U.S. patents 5,932,558; 6,020,321; 6,555,545; 7,795,427; adenosine A_1R and A_{2B}R antagonists to treat fatty liver (pending); adenosine A_{2A}R agonists to prevent prosthesis loosening (pending). B.N.C. is a consultant for Bristol-Myers Squibb (New York, NY, USA), Novartis (New York, NY, USA), CanFite Biopharmaceuticals (Petah-Tikva, Israel), Cypress Laboratories (Allen, TX, USA), Regeneron (Westat, DSMB; Tarrytown, NY, USA), Endocyte (West Lafayette, IN, USA), Protalex (Florham Park, NJ, USA), Allos, Inc. (Westminster, CO, USA), Savient (East Brunswick Township, NJ, USA), Gismo Therapeutics (Howard Beach NY, USA), Antares Pharmaceutical (Ewing, NJ, USA), Medivector (Boston, MA, USA), King Pharmaceutical (Bristol, TN, USA), Celizome (St. Petersburg, FL, USA), Tap Pharmaceuticals (Lake Forest, IL, USA), Prometheus Laboratories (Lake Forest, IL, USA), Sepracor (Basel, Switzerland), Amgen (Thousand Oaks, CA, USA), Combinatorx (Boston, MA, USA), Kyowa Hakka (Tokyo, Japan), Hoffman-LaRoche (Basel, Switzerland), and Avidimer Therapeutics (Ann Arbor, MI, USA). B.N.C. has stock in CanFite Biopharmaceuticals. Author contributions: B.C. and A.M. designed most of the experiments; A.M. was the primary person responsible for carrying out all experimental procedures; and M.P.A. helped with Western blot experiments.

REFERENCES

1. Suda, T., Takahashi, N., Udagawa, N., Jimi, E., Gillespie, M. T., and Martin, T. J. (1999) Modulation of osteoclast differentiation and function by the new members of the tumor necrosis factor receptor and ligand families. *Endocr. Rev.* **20,** 345–357
2. Manolagas, S. C. (2000) Birth and death of bone cells: basic regulatory mechanisms and implications for the pathogenesis and treatment of osteoporosis. *Endocr. Rev.* **21,** 115–137
3. Teitelbaum, S. L. (2000) Bone resorption by osteoclasts. *Science* **289,** 1504–1508
4. McHugh, K. P., Shen, Z., Crotti, T. N., Flannery, M. R., Fajardo, R., Bierbaum, B. E., and Goldring, S. R. (2007) Role of cell-matrix interactions in osteoclast differentiation. *Adv. Exp. Med. Biol.* **602,** 107–111
5. Takayanagi, H. (2007) Osteoimmunology: shared mechanisms and crosstalk between the immune and bone systems. *Nat. Rev. Immunol.* **7,** 292–304
6. Yoshida, H., Hayashi, S., Kunisada, T., Ogawa, M., Nishikawa, S., Okamura, H., Sudo, T., and Shultz, L. D. (1990) The murine mutation osteopetrosis is in the coding region of the macrophage colony stimulating factor gene. *Nature* **345,** 442–444
7. Yasuda, H., Shima, N., Nakagawa, N., Yamaguchi, K., Kinosaki, M., Mochizuki, S., Tomoyasu, A., Yano, K., Goto, M., Murakami, A., Tsuda, E., Morinaga, T., Higashio, K., Udagawa, N., Takahashi, N., and Suda, T. (1998) Osteoclast differentiation factor is a ligand for osteoprotegerin/osteoclastogenesis-inhibitory factor and is identical to TRANCE/RANKL. *Proc. Natl. Acad. Sci. U. S. A.* **95,** 3597–3602
8. Simonet, W. S., Lacey, D. L., Dunstan, C. R., Kelley, M., Chang, M. S., Luthy, R., Nguyen, H. Q., Wooden, S., Bennett, L., Boone, T., Shimamoto, G., DeRose, M., Elliott, R., Colombero, A., Tan, H. L., Trail, G., Sullivan, J., Davy, E., Bucay, N., Renshaw-Gegg, L., Hughes, T. M., Hill, D., Pattison, W., Campbell, P., Sander, S., Van, G., Tarpley, J., Derby, P., Lee, R., and Boyle, W. J. (1997) Osteoprotegerin: a novel secreted protein involved in the regulation of bone density. *Cell* **89,** 309–319
9. Dougall, W. C., Glaccum, M., Charrier, K., Rohrbach, K., Brasel, K., De Smedt, T., Daro, E., Smith, J., Tometsko, M. E., Maliszewski, C. R., Armstrong, A., Shen, V., Bain, S., Cosman, D., Anderson, D., Morrissey, P. J., Peschon, J. J., and Schuh, J. (1999) RANK is essential for osteoclast and lymph node development. *Genes Dev.* **13,** 2412–2424
10. Li, J., Sarosi, I., Yan, X. Q., Morony, S., Capparelli, C., Tan, H. L., McCabe, S., Elliott, R., Scully, S., Van, G., Kaufman, S., Juan, S. C., Sun, Y., Tarpley, J., Martin, L., Christensen, K., McCabe, J., Kostenuik, P., Hsu, H., Fletcher, F., Dunstan, C. R., Lacey, D. L., and Boyle, W. J. (2000) RANK is the intrinsic hematopoietic cell surface receptor that controls osteoclastogenesis and regulation of bone mass and calcium metabolism. *Proc. Natl. Acad. Sci. U. S. A.* **97,** 1566–1571

11. Breckler, M., Berthouze, M., Laurent, A. C., Crozatier, B., Morel, E., and Lezoualc'h, F. (2011) Rap-linked cAMP signaling Epac proteins: compartmentation, functioning and disease implications. *Cell. Signal.* **23,** 1257–1266
12. Kondo, H., Guo, J., and Bringhurst, F. R. (2002) Cyclic adenosine monophosphate/protein kinase A mediates parathyroid hormone/parathyroid hormone-related protein receptor regulation of osteoclastogenesis and expression of RANKL and osteoprotegerin mRNAs by marrow stromal cells. *J. Bone Miner. Res.* **17,** 1667–1679
13. De Rooij, J., Zwartkruis, F. J., Verheijen, M. H., Cool, R. H., Nijman, S. M., Wittinghofer, A., and Bos, J. L. (1998) Epac is a Rap1 guanine-nucleotide-exchange factor directly activated by cyclic AMP. *Nature* **396,** 474–477
14. Gloerich, M., and Bos, J. L. (2010) Epac: defining a new mechanism for cAMP action. *Annu. Rev. Pharmacol. Toxicol.* **50,** 355–375
15. Ster, J., De Bock, F., Guerineau, N. C., Janossy, A., Barrere-Lemaire, S., Bos, J. L., Bockaert, J., and Fagni, L. (2007) Exchange protein activated by cAMP (Epac) mediates cAMP activation of p38 MAPK and modulation of Ca2+-dependent K+ channels in cerebellar neurons. *Proc. Natl. Acad. Sci. U. S. A.* **104,** 2519–2524
16. Soysa, N. S., and Alles, N. (2009) NF-kappaB functions in osteoclasts. *Biochem. Biophys. Res. Commun.* **378,** 1–5
17. Yoon, S. H., Ryu, J. Y., Lee, Y., Lee, Z. H., and Kim, H. H. (2010) Adenylate cyclase and calmodulin-dependent kinase have opposite effects on osteoclastogenesis by regulating the PKA-NFATc1 pathway. *J. Bone Miner. Res.* **26**(6), 1217–1229
18. Takada, K., Kajiya, H., Fukushima, H., Okamoto, F., Motokawa, W., and Okabe, K. (2004) Calcitonin in human odontoclasts regulates root resorption activity via protein kinase A. *J. Bone Miner. Metab.* **22,** 12–18
19. Granholm, S., Lundberg, P., and Lerner, U. H. (2007) Calcitonin inhibits osteoclast formation in mouse haematopoetic cells independently of transcriptional regulation by receptor activator of NF-κB and c-Fms. *J. Endocrinol.* **195,** 415–427
20. Park, Y. G., Kim, Y. H., Kang, S. K., and Kim, C. H. (2006) cAMP-PKA signaling pathway regulates bone resorption mediated by processing of cathepsin K in cultured mouse osteoclasts. *Int. Immunopharmacol.* **6,** 947–956
21. Mediero, A., Perez-Aso, M., and Cronstein, B. N. (2013) Activation of adenosine A2A receptor reduces osteoclast formation via PKA- and ERK1/2-mediated suppression of NFkappaB nuclear translocation. *Br. J. Pharmacol.* **169,** 1372–1388
22. Zou, W., Izawa, T., Zhu, T., Chappel, J., Otero, K., Monkley, S. J., Critchley, D. R., Petrich, B. G., Morozov, A., Ginsberg, M. H., and Teitelbaum, S. L. (2013) Talin1 and Rap1 are critical for osteoclast function. *Mol. Cell. Biol.* **33,** 830–844
23. Guerrini, M. M., Sobacchi, C., Cassani, B., Abinun, M., Kilic, S. S., Pangrazio, A., Moratto, D., Mazzolari, E., Clayton-Smith, J., Orchard, P., Coxon, F. P., Helfrich, M. H., Crockett, J. C., Mellis, D., Vellodi, A., Tezcan, I., Notarangelo, L. D., Rogers, M. J., Vezzoni, P., Villa, A., and Frattini, A. (2008) Human osteoclast-poor osteopetrosis with hypogammaglobulinemia due to TNFRSF11A (RANK) mutations. *Am. J. Hum. Genet.* **83,** 64–76
24. Roelofs, A. J., Coxon, F. P., Ebetino, F. H., Lundy, M. W., Henneman, Z. J., Nancollas, G. H., Sun, S., Blazewska, K. M., Bala, J. L., Kashemirov, B. A., Khalid, A. B., McKenna, C. E., and Rogers, M. J. (2010) Fluorescent risedronate analogues reveal bisphosphonate uptake by bone marrow monocytes and localization around osteocytes in vivo. *J. Bone Miner. Res.* **25,** 606–616
25. Frith, J. C., Monkkonen, J., Auriola, S., Monkkonen, H., and Rogers, M. J. (2001) The molecular mechanism of action of the antiresorptive and antiinflammatory drug clodronate: evidence for the formation in vivo of a metabolite that inhibits bone resorption and causes osteoclast and macrophage apoptosis. *Arthritis Rheum.* **44,** 2201–2210
26. Mediero, A., Kara, F. M., Wilder, T., and Cronstein, B. N. (2012) Adenosine A(2A) receptor ligation inhibits osteoclast formation. *Am. J. Pathol.* **180,** 775–786.
27. Yasuda, H., Shima, N., Nakagawa, N., Yamaguchi, K., Kinosaki, M., Goto, M., Mochizuki, S. I., Tsuda, E., Morinaga, T., Udagawa, N., Takahashi, N., Suda, T., and Higashio, K. (1999) A novel molecular mechanism modulating osteoclast differentiation and function. *Bone* **25,** 109–113
28. Chitu, V., Pixley, F. J., Macaluso, F., Larson, D. R., Condeelis, J., Yeung, Y. G., and Stanley, E. R. (2005) The PCH family member MAYP/PSTPIP2 directly regulates F-actin bundling and enhances filopodia formation and motility in macrophages. *Mol. Biol. Cell* **16,** 2947–2959
29. Pfaffl, M. W. (2001) A new mathematical model for relative quantification in real-time RT-PCR. *Nucleic Acids Res.* **29,** e45
30. Franzoso, G., Carlson, L., Xing, L., Poljak, L., Shores, E. W., Brown, K. D., Leonardi, A., Tran, T., Boyce, B. F., and Siebenlist, U. (1997) Requirement for NF-kappaB in osteoclast and B-cell development. *Genes Dev.* **11,** 3482–3496
31. Shahrara, S., Castro-Rueda, H. P., Haines, G. K., and Koch, A. E. (2007) Differential expression of the FAK family kinases in rheumatoid arthritis and osteoarthritis synovial tissues. *Arthritis Res. Ther.* **9,** R112
32. Yu, M., Qi, X., Moreno, J. L., Farber, D. L., and Keegan, A. D. (2011) NF-kappaB signaling participates in both RANKL- and IL-4-induced macrophage fusion: receptor cross-talk leads to alterations in NF-kappaB pathways. *J. Immunol.* **187,** 1797–1806
33. Chen, H., Wild, C., Zhou, X., Ye, N., Cheng, X., and Zhou, J. (2013) Recent advances in the discovery of small molecules targeting exchange proteins directly activated by cAMP (EPAC). *J. Med. Chem.* **57,** 3651–3665
34. Sugimoto, N., Miwa, S., Ohno-Shosaku, T., Tsuchiya, H., Hitomi, Y., Nakamura, H., Tomita, K., Yachie, A., and Koizumi, S. (2011) Activation of tumor suppressor protein PTEN and induction of apoptosis are involved in cAMP-mediated inhibition of cell number in B92 glial cells. *Neurosci. Lett.* **497,** 55–59
35. Blair, H. C., Robinson, L. J., and Zaidi, M. (2005) Osteoclast signalling pathways. *Biochem. Biophys. Res. Commun.* **328,** 728–738
36. Soysa, N. S., Alles, N., Shimokawa, H., Jimi, E., Aoki, K., and Ohya, K. (2009) Inhibition of the classical NF-kappaB pathway prevents osteoclast bone-resorbing activity. *J. Bone Miner. Metab.* **27,** 131–139
37. Saltel, F., Chabadel, A., Bonnelye, E., and Jurdic, P. (2008) Actin cytoskeletal organisation in osteoclasts: a model to decipher transmigration and matrix degradation. *Eur. J. Cell Biol.* **87,** 459–468
38. Croke, M., Ross, F. P., Korhonen, M., Williams, D. A., Zou, W., and Teitelbaum, S. L. (2011) Rac deletion in osteoclasts causes severe osteopetrosis. *J. Cell Sci.* **124,** 3811–3821
39. Ory, S., Munari-Silem, Y., Fort, P., and Jurdic, P. (2000) Rho and Rac exert antagonistic functions on spreading of macrophage-derived multinucleated cells and are not required for actin fiber formation. *J. Cell Sci.* **113**(Pt. 7), 1177–1188
40. Ray, B. J., Thomas, K., Huang, C. S., Gutknecht, M. F., Botchwey, E. A., and Bouton, A. H. (2012) Regulation of osteoclast structure and function by FAK family kinases. *J. Leukoc. Biol.* **92,** 1021–1028
41. Yamamoto, Y., Noguchi, T., and Takahashi, N. (2005) Effects of calcitonin on osteoclast. *Clin. Calcium* **15,** 147–151
42. Lee, Y. J., Kim, M. O., Ryu, J. M., and Han, H. J. (2012) Regulation of SGLT expression and localization through Epac/PKA-dependent caveolin-1 and F-actin activation in renal proximal tubule cells. *Biochim. Biophys. Acta* **1823,** 971–982
43. Grandoch, M., Roscioni, S. S., and Schmidt, M. (2010) The role of Epac proteins, novel cAMP mediators, in the regulation of immune, lung and neuronal function. *Br. J. Pharmacol.* **159,** 265–284

Received for publication April 15, 2014.
Accepted for publication July 21, 2014.